Photoinduced Irreversible Effects on Magnetic Properties and Allied Phenomena in Magnetic Oxides. II

K. Hisatake, I. Matsubara, K. Maeda, *T. Fujihara and **S. Kainuma

Department of Physics and *Chemistry,
Kanagawa Dental College,
Yokosuka, Kanagawa 238 Japan
**Department of Electrical Engineering,
Asikaga Institute of Technology
Ashikaga, Gunma 326 Japan

I. Introduction

In the preceding review article of this series, the simple survey of photoinduced magnetic effect on yttrium iron garnet (YIG), the experimental procedure and lists of the authors were described. This review concerns with the main theme and intimately related problems as follows; after effects connected with induced anisotropy, wall pinning by anisotropic ferrous ions and optical absorption mechanism.

II. Photoinduced Magnetic Effects and Related Phenomena

2. 1 After Effect Associated With Induced Anisotropy

As mentioned in the introduction, PME seems to be strongly correlated with the magnetic anneal or induced anisotropy also in the dark. Thus the authors will treat it in more detail, especially where Fe^{2+} or Co^{2+} ions are involved in magnetic oxides. When a ferromagnetic crystal is annealed in a sufficiently strong magnetic field at a certain temperature lower than Curie point and then cooled, an additional anisotropy sometimes is caused.[2] This induced anisotropy energy, superposed on the other magnetic anisotropies, is given by

$$E_{1A} = -F(\alpha_1^2\beta_1^2 + \alpha_2^2\beta_2^2 + \alpha_3^2\beta_3^2) - G(\alpha_1\alpha_2\beta_1\beta_2 + \alpha_1\alpha_3\beta_1\beta_3 + \alpha_2\alpha_3\beta_2\beta_3) \qquad (2.\ 1)$$

where α_1, α_2, α_3 are the direction cosines of the magnetization during annealing and β_1, β_2, β_3 are likewise during the measurement of the anisotropy energy. For a polycrystalline material the induced anisotropy has a uniaxial character and can be written as

$$E_{1A} = -K_u \cos^2\theta \qquad (2.\ 2)$$

where θ is the angle between the direction of the magnetization during the measurement and that during the annealing treatment. There are many possible mechanisms for an induced anisotropy. The most important mechanism is the preferential location of atoms or orientation of atom pairs. The authors will now consider the case of the preferential location of atoms. Preferential location of single atoms is caused by the

fact that different sites have different energies with respect to the direction of the magnetization. The energy of a certain site i can mostly be described as

$$e_i = w\ (\cos^2 \theta_i - 1/3) \tag{2. 3}$$

where θ_i is the angle between the direction of the magnetic moment of the atom or ion and the local symmetry axis and w is the difference between maximum and minimum energy. The factor 1/3 is added to make the average energy over all angles 0. Consider a single crystal with n groups of sites, each group having a common symmetry axis. In the case of octahedral sites in the spinel or garnet structure, $n=4$ with four different [111] directions as shown in Fig. 2. 1. Assume that there are N atoms per unit volume distributed over the available sites according to a Boltzmann distribution. If $e_i \ll kT$, the equilibrium concentration of atoms on site i is found by calculation to be given by

$$C_{i0} = N/n\ (1-e_i/kT) \tag{2. 4}$$

It should be noted that e_i is dependent of temperature. When the thermal annealing is carried out at a temperature T' and the equilibrium distribution of this temperature is frozen in at a lower temperature T, the following relation for the induced anisotropy energy is obtained,

$$E_{1A} = \sum_{i=1}^{n} C_{i0}\ (T')\ e_i\ (T) \tag{2. 5}$$

From eqs. (2. 3), (2. 4) and (2. 5), it follows that

$$E_{1A} = -(N/n\ kT') \sum_{i=1}^{n} w\ (T')\ w\ (T)\ (\cos^2 \theta'_i - 1/3)\ (\cos^2 \theta_i - 1/3) \tag{2. 6}$$

Now F and G of eq. (2. 1) can be expressed by

$$F = f_F\ (N/kT')\ w\ (T)\ w\ (T') \tag{2. 7}$$

and

$$G = g_G\ (N/kT')\ w\ (T)\ w\ (T') \tag{2. 8}$$

where f_F and g_G are constants determined by geometrical factors such as the direction of the local symmetry axis. For the isotropic case we find that

$$K_U = 2/15\ (N/kT')\ w\ (T)\ w'\ (T') \tag{2. 9}$$

The equations (2. 5) to (2. 9) were derived for a thermal equilibrium distribution at temperature T'. The time needed to attain the equilibrium state may be important for the after effect and problems in this review. Transitions of an atom from a certain site i to another site j caused by lattice vibrations, occurs with a certain activation energy $E-e_i$, where E is the maximum energy of the atom during its jump. This situation is schematically given in Fig. 2. 2. The jump frequency is

$$\nu_i = \nu_0 \exp\ [-(E-e_i)\ /kT] \tag{2. 10}$$

For a jump from the $n-1$, j-sites to the i-sites the same equations can be used with e_i replaced by e_j. From the expressions for the jump frequencies one can calculate the rate of change of the concentration C_i as

$$\frac{dC_i}{dt} = -\frac{n}{n-1}\ (C_i - C_{i0})\ \nu_0 \exp\ \left(-\frac{E}{kT}\right) \tag{2. 11}$$

The change of C_i with time can be written as

$$C_i = C_{i0}\ \left[1-\exp\ \left(-\frac{t}{\tau}\right)\right] \tag{2. 12}$$

From (2. 11) and (2. 12), a relaxation time τ is expressed as

$$\tau = -\frac{n-1}{n}\ \frac{1}{\nu_0}\exp\left(\frac{E}{kT}\right) = \tau_0 \exp\left(\frac{E}{kT}\right) \qquad (2.\ 13)$$

As a consequence of the time dependence of C_i the induced anisotropy is also time dependent with the same relaxation time. It should be noted that the energy E may vary a little due to the presence of irregularities in the crystal lattice. Since the relaxation time varies exponentially with E, these small variations may lead to a wide distribution of relaxation times. The induced anisotropies are large when highly anisotropic ions are involved, e. g. Fe^{2+} or Co^{2+} in spinel or garnet ferrites. The authors will now discuss the phenomena observed in these situations. The main phenomena connected with the induced anisotropy and its relaxation will be mentioned, since the photoinduced effects may be correlated with them as mentioned before. Various types of phenomena, or after effects are tentatively summarized as follows.

a) Induced anisotropy and its relaxation ; the additional torque due to magnetic anneal and its temporal variation after rotation of the applied field.[3,4]

b) Rotational hysteresis ; the damping of uniform rotation of the sample caused by the torque of induced anisotropy.[5,6]

c) Ferromagnetic resonance line broadening ; the damping of uniform precession ; maxima on line width versus temperature of which positions are frequency dependent.[7,8]

d) Disaccommodation of permeability ; the time decrease of permeability after demagnetization due to the stabilization of the Bloch walls.[9,10]

e) Accommodation of permeability ; in contrast to disaccommodation, the time increase of permeability after demagnetization due to the destabilization of the Bloch walls.[11~14]

f) Magnetic viscocity ; the time increase of magnetization after applying magnetic field also due to gradual destabilization of the Bloch walls.[15,16]

g) Time change of hysteresis curve ; the stabilization and destabilization of the magnetization orientation and its influence on irreversible magnetization process.[17,18]

h) Magnetic losses in ac fields ; the damping of wall motion or maxima in the dependence of tan δ on frequency and temperature.[19~21]

These phenomena may be classified into two types. The first three ones concern with the homogeneous magnetization and the induced anisotropy may be taken as constant throughout all their volume. The rest are correlated with the effect of stabilization of Bloch walls and or magnetic domains. Through studying these phenomena, we can obtain some important informations i. e., the local order and its origin and the magnitudes of the anisotropic coupling, the kinetics and mechanisms of the underlying relaxation process, and effects of induced anisotropy on magnetization process. From another point of view, the phenomena can be divided into two groups also : (A) ionic process and (B) electronic process. An ionic process is characterized by the change of ionic distribution while during an electronic process ions essentially retain their lattice positions and only small displacements are allowed. The distinction between these two kinds of processes is usually based on the experimental knowledge of the activation energy from (2. 13). For ionic processes the activation energy is higher, typically 1 eV and they are as a rule observable only at high temperatures. A direct observation of induced anisotropy, its relaxation and the disaccommodation of permeability have been

most often used for their study. In this problem many physicists in our country have done to not a few contrributions. As found from the analysis of the experimental results in substances containing various concentrations of vacancies, these role may be divided into the two ones ; Iida mechanism[22,23] and Ohta mechanism.[10] First the presence of cation vacancies is able to facilitate the diffusion of the active ions. For a certain range of vacancy concentration the relaxation times at constant temperature are then inversely proportional to their concentration.[23] Second, on the other hand, the vacancies are assumed to be the source of the induced anisotropy either separately or in the form of pair and more complex configurations with some kind of ions in order to explain the experimental result that the magnitude of induced anisotropy itself is governed by the concentration of vacancies.[10] This behavior has been found in iron rich ferrites for the induced anisotropy relaxation observed around room temperature. In this context, Yanase calculated the dipole-dipole contribution to the anisotropy energy.[24] Using Fourier transformotions, he obtained

$$E_{\mathrm{dip}} = A_{\mathrm{dip}}\, N_{\mathrm{m}}\, m\,(m-m')\ (\alpha_1\alpha_2 + \alpha_2\alpha_3 + \alpha_3\alpha_1). \qquad (2.\ 14)$$

The equation represents the dipolar anisotropy energy of trigonal symmetry with respect to the chosen [111] direction. N is the number of octahedral sites per unit volume, m and m' are the averrage magnetic moments in the [111] sites and the remaining ones respectively and A_{dip} is determined using the values of geometrical parameters as $A_{\mathrm{dip}} = 4 \times 10^{-18}$ erg cm^{-3}. The equilibrium distribution of vacancies at the given temperature is then found by minimizing the free energy

$$f = E_{\mathrm{dip}} - TS. \qquad (2.\ 15)$$

As a result, induced anisotropy of a G type is drawn as

$$G\,(T_{\mathrm{a}},\ T) = (16N_{\mathrm{v}}\ A_{\mathrm{dip}}{}^2/kT)\ (gS)^4\,[M\,(T)\,/M\,(0)\,]^2 \qquad (2.\ 16)$$

where N_{v} is the number of vacancies per cubic centimeter, Ta and T are the temperature of annealing and measurement respectively and gS the average magnetic moment. Thus, Ohta mechanism seems to be confirmed theoretically. However, the authors would not like to believe that this problem has been completely established. And it will need more detailed experiment to attain the final conclusion. Again we will discuss the role of vacancies in PME on YIG. In order to observe a PME in high temperature, it seems necessary to study the induced anisotropy at high temperatures in more detailed way. The anisotropic effect of Co^{2+} ions outweighs all the other possible contributions to the induced anisotropy, which has been strongly correlated with PME.[25~27] Consequently, the authors discuss it in other sections along with experimental results. The electronic processes are as a rule connected with a redistribution of the electrical charges of the cations. This process of charge transfer is basically the same as the mechanism of electrical conductivity in magnetic oxides, where the hopping model is often taken as adequate. The coincidence of activation energies for both these phenomena found in many cases justifies the assumption about their common origin. The most common example of relaxation phenomena connected with valency exchange concerns electron jumps between Fe^{2+} and Fe^{3+} [28,29], while other ions as Co, Mn, Ni, Cu[9] etc may be thought to display a similar behavior. Unfortunately, the direct evidence has, however, not been obtained. A small value of activation energy (0.1 eV) is found, if the electrons jump short ranges and if the transrational symmetry of the lattice is

not heavily perturbed. If, however, the concentration of the exchangnig ions is too low for electrons to hop easily, i. e., separated by a certain number of ions of a different kind, the activation energy of the electron transfer may be considerably higher (~ 0.5 eV).[30] In order to consider the details of the diffusion mechanism, R. P. Hunt[5] adopted the point of view that an electron is transfered from one octahedral site to another through an activated jump over an intervening potential barrier. Mapping the potential between each type of site into a plane may result in the situation shown in Fig 2. 2. The energy of the bottom of the i-th well, i (θ_i), is given by Eq. 2. 2. For simplicity the potential peaks are fixed at E_b of the potential barrier. The number of jumping from well 2 to well 3 will be assumed to be proportional to the product of the Boltzmann factor and the number of particles actually occupying well 2. Thus the net rate of change of the particles in the i-th ($i=1, 2, 3, 4$) sites, n_i is expressed in a matrix equation as follows,

$$\begin{bmatrix} \dot{n}_1 \\ \dot{n}_2 \\ \dot{n}_3 \\ \dot{n}_4 \end{bmatrix} = \begin{bmatrix} -3e^{\beta E_1} & e^{\beta E_2} & e^{\beta E_3} & e^{\beta E_4} \\ e^{\beta E_1} & -3e^{\beta E_2} & e^{\beta E_3} & e^{\beta E_4} \\ e^{\beta E_1} & e^{\beta E_2} & -3e^{\beta E_3} & e^{\beta E_4} \\ e^{\beta E_1} & e^{\beta E_2} & e^{\beta E_3} & -3e^{\beta E_4} \end{bmatrix} \cdot \begin{bmatrix} n_1 \\ n_2 \\ n_3 \\ n_4 \end{bmatrix} \qquad (2.\ 18)$$

where $\beta = 1/kT$ and $\nu = \nu_0 e^{-\beta E_b}$.

The more detailed rate equation has been proposed dy Wurlitzer[31] in PME, as not described here. The activation energy, On the other hand, in an ionic process may be lowered, if the vacancy is involved considerably. Correspondinly, definite conclusions on this problem remains vague. A different type of an electronic process may be based on the effect of Jahn-Teller distortions.[32] In the case of orbital degeneracy, the distribution of the outer electrons among d orbitals of the given ion is coupled to the positions axis also changes the electron distribution and the inverse process may take place also. Specifically Mn^{3+} or Cu^{2+} ions in octahedral coordination tend to distort tetragonally the surrounding anion octahedron, the positions of the energy levels being dependent upon the mutual orientation of magnetization and the distortion axis. The observation of such a type of relaxation phenomenon is actually often conditioned by the stabilization of the distortion axis by an extra electron. This may be the case for the relaxation spectra of Mn-Fe spinels.[32] For example, nickel ferrite is an inverse spinel where the nickel is predominantly on the octahedral sites.[16] Ni^{2+} ions cause no distortion of these sites. If some nickel ions, however, appear on the tetrahedral sites, these sites will undergo Jahn-Teller distortions. In such distortions the oxygens forming the tetrahedron shift slightly change the symmetry from cubic to tetragonal. In the absence of a magnetic field, the tetragonal distortions considered here have three equivalent directions, one along each of the cube axes. It has been known that a Ni^{2+} ion in a distorted tetrahedral site has a substantial magnetic anisotropy.[33] Consequently, an applied field will make one of the three possible directions of distortion energetically favourable. Then, at equilibrium, the directions of the Jahn-Teller distortion from one axis to

another cannot be predicted accurately. Therefore, an accurate determination of validity of the model may not be compared with other models. In addition, it is possible that their observed effect is not only due to isolated sites but also to the interaction of a number of nickel ions on neighboring tetrahedral sites. If the interactions between neibouring ions are important, we have the possibility of a cooperative phenomenon, that is, in some region of the material all the distortions are in the same direction. In this case the decrease of entropy by ordering will increase the activation energy, associated with a change of the distortion from one crystal axis to another. In the case of Mn Zn ferrite, tetragonal distortions within the spinel lattice are to be expected if Mn^{3+} is present in sufficient quantity, a cooperative Jahn-Teller distortion occurs, and the crystal is macroscopically tetragonal. In these kinds of samples, one of the authors tried to carry out the measurement of PME but found no effect as seen in Si-YIG.[35] If this mechanism applies equally well to YIG (Mn, Cu, Ni), PME will be explained through a simple equation of hole release ;

$$Mn^{2+} + h\nu \longrightarrow Mn^{3+} + \text{(electron trapped with the unspecifled traps)}$$

Thus, it will be reasonable that the domain wall may be pinned down in these circumstance of right-hand term. For the first time, one of the authors (K. H) introduced this idea in order to give an explanation of PME in YIG (Mn, Cu or Ni) previously as shown in Fig. 2. 3.[34,35] It is, however, needed to study furthermore in order that this picture will be completely established.

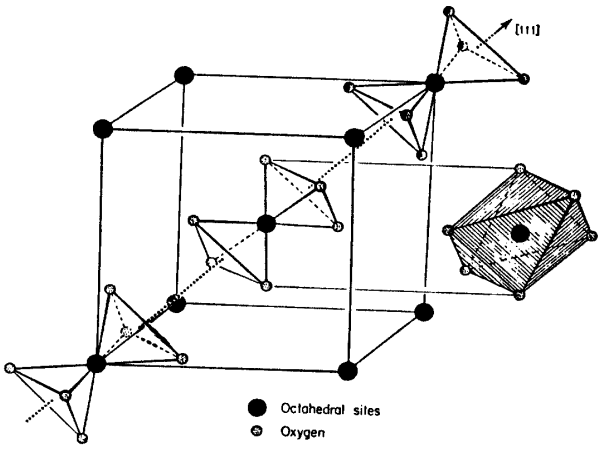

Fig. 2. 1. One eighth unit cell showing the trigonal disposition of the oxygen ions for one of the four [111] symmetry axes. Center site duplicated at right to show slightly distorted octahedral configuration[5]

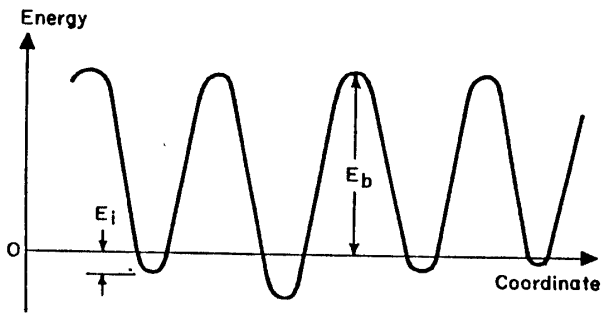

Fig. 2. 2. One-diminsional potential barrier scheme.[5]

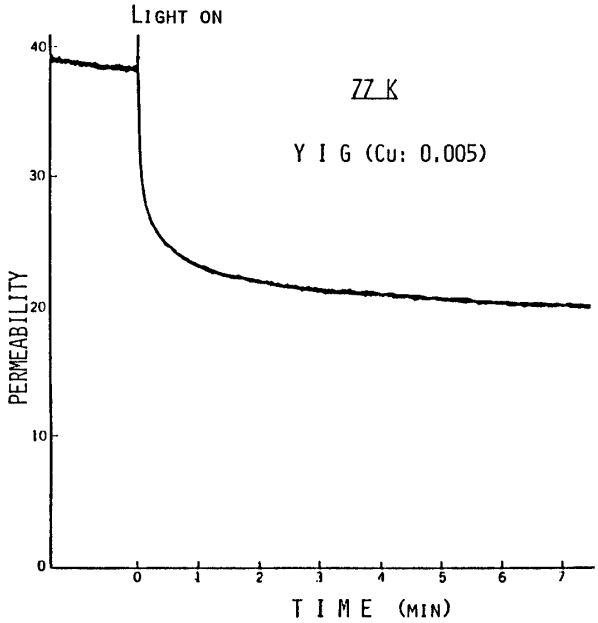

Fig. 2. 3 Time dependence of initial permeability on illumination.[35]

References

1. J. C. Slonczewski : "Magnetism I" (Academic Press, New York, 1963).
2. L. Neel : J. Phys. Radium 13 (1952) 249.
3. K. Ohta : "Foundation of Magnetics" (Kyoritu, Toko, 1973) (Japanese)
4. K. Ohta and T. Yamadaya : J. Phys. Soc. Japan SB-I (1962) 291.
5. R. P. Hunt : Tech. Rept. 199, Lab Inst. Res. M. I. T. (1965).
6. A. Broes van Groenou, J. L. Page and R. F. Pearson : J. Phys. Chem. Solids 28 (1967) 1017.
7. A. M. Clogston : Bell. System. Tech. J., 34 (1955) 739.
8. A. Broes van Groenou, P. F. Bongers and A. L. Stuyts : Mater. Sci. Eng., 3 (1968/69) 317.
9. U. Enz : Physica 27 (1958) 609.
10. K. Ohta : J. Phys. Soc. Japan 16 (1961) 250.
11. A. Marais, T. Merceron and M. Porte : IEEE Trans. Mag-8 (1972) 685.
12. S. Kainuma and K. Hisatake : Jpn. Appl. Phys. 16 (1977) 183.
13. K. Hisatake and J. A. R. Jordao : J. M. C. 1 (1981) 161.
14. K. Hisatake and J. A. R. Jordao : J. M. C. 2 (1982) 103.
15. L. Neel : J. Phys. Radium 13 (1952) 249.
16. J. Smit and H. P. J. Wijn : Ferrites (Int. Edition, Philips Tech. Lib., 1965)
17. J. F. Janak : J. Appl. Phys. 34 (1963) 1119.
18. K. Hisatake, I. Matsubara, K. Maeda, T. Fujihara, I. Sasaki and T. Nakano : To be published in J. Elec. Mech. Ind. Assoc. Jpn. (Special Issue, 1987).
19. M. Wurlitzer and M. Richter : phys. stat. sol. (a) 3 (1970) K211.
20. M. Wurlitzer : phys. stat. sol. (a) 78 (1983) K87.
21. F. Brown and C. L. Gravel : Phys. Rev. 97 (1955) 55.
22. S. Iida : and H. Miwa : J. Phys. Soc. Japan 21 (1966) 2505.
23. S. Iida : Ferrites I (Proc. Int. Conf. Ferrites, Kyoto. 1970) p. 17.
24. A. Yanase : J. Phys. Soc. Japan 17 (1962) 1005.
25. F. K. Lotgering : J. Phys. Chem. Solids 36 (1975) 1183.
26. K. Hisatake : phys. stat. sol. (a) 3 (1976) K131.
27. K. Hisatake and K. Ohta : J. de Physique 38 (1977) 219.
28. S. J. Pickart and A. C. Turnock : J. Phys. Chem. Solids 10 (1959) 242.
29. A. K. Goswami, M. Rosenbloom and R. W. Teal : J. J. Appl. Phys. 39 (1966) 1303.
30. K. Zaveta, E. I. Trinkler and F. Zounova : Phys. Seat. Sol. 14 (1966) K9.
31. M. Wurlitzer : Acta Phys. Slov., 34 (1984) 177.
32. F. J. Schnettler and E. M. Gyorgy : J. Appl. Phys. 35 (1964) 330.
33. P. K. Baltzer : J. Phys. Soc. Japan 17 Suppl. B-I (1962) 192.
34. K. Hisatake : Trans. IECE 58C (1975) 27.
35. K. Hisatake and K. Hirasaki : Trans. IECE 58C (1975) 160.

2. 1. 2 Wall Pinning by Anisotropic Ferrous ions

The change of permeability by ordering of anisotropic ions such as Fe^{2+} and Co^{2+} ions in a domain wall can be easily calculated using the following model, in which the problem is reduced to its most simple form.[1,2] We consider a 180° wall with thickness parallel to the xz plane in a uniaxial material having the easy direction of magnetization along the c-axis (z-direction). The uniaxial anisotropic ions are assumed to occur on sites with easy direction either along the x-axis or along the z-axis and they will occupy a small fraction of these two kinds of otherwise equivalent sites. Then the energy difference between ions on the two kinds of sites depends on the magnetization

direction, which is a function of the position η along the y-axis in the wall, so that a Boltzmann distribution is unchanged and does not fit in the new wall position. The energy difference ΔE_{anis} per cm^2 wall (pinning energy) for a small wall displacement y can be calculated straight-forwardly in the approximation that the turning angle is assumed to increase linearly with the distance in the wall[3] and for $kT \gg$ ionic anisotropy. Hence

$$E_{\text{anis}} = (\pi \varepsilon^2 \, n y^2) \; (4 \, kT\delta)^{-1} = 0.5 f y^2 \qquad (2.\ 20)$$

where n is the number of hard ions per cm^{-3}, ε is the ionic anisotropy constant defined by $\varepsilon \sin^2 \theta$ for the local, uniaxial anisotropy energy and f is the stiffness constant arising form pinning. This leads to a susceptibility decrease of

$$(\Delta \chi^{-1}) \text{ cm}^2 \text{ wall} = \Delta \, (d\text{x})^{-1} \text{ cm} = \text{f}/(4M_s^2) \qquad (2.\ 21)$$

where M_s is the saturation magnetization and d is the mean distance between the 180° walls. For $\mu \gg 1$,

$$\Delta \mu_{\text{sat}}{}^{-1} = \mu_{\text{sat}}{}^{-1} - \mu_{\text{g}}{}^{-1} = (4\pi)^{-1} \; \Delta \chi^{-1} = \text{df} \; (16 \pi \, M_s^2) = \text{d} \eta \varepsilon \; (32 M_s^2 \, \delta) \varepsilon (\, kT)^{-1} \qquad (2.\ 22)$$

Equation 2. 22 is derived for thermal equilibrium in the wall and is therefore not applicable to PME. It may be, however, applicable to DA (disaccommodation) during saturation process starting from the demagnetized state. The DA at 77 K of YIG sample in fig. 2. 3 may be attributed to Fe^{2+} ions. If the concentration of 0.005 Fe^{2+} ion is assumed and the eightfold mutual coordination of octahedral sites is considered, this corresponds to 4×10^{17} cm^{-3}. Further putting $d = 10^{-3}$ cm, $\delta = 500$A, $M_s = 190$ gauss, the experimental value of $\Delta \mu_{\text{sat}}{}^{-1} = 0.04$ for DA is then estimated to be 40 cm^{-1} per Fe^{2+}. This value obtained above has the expected order of magnitude. In a weakly anisotropic material such as YIG doped with strongly anisotropic ions like Fe^{2-} so far discussed,[4] domain walls may be pinned by concentration fluctuations of the hard ions that are immobil and distributed at random. A semiquantitative equation may be derived using the simplified model of the wall. A concentration fluctuation in a certain volume that are too small or large in size with respect to the wall thickness δ may not provide wall pinning. The pinning due to concentration fluctuation in a certain volume of the order of δ^3 may be estimated by dividing the wall into cubes with an edge δ so that the wall surface is divided into square fragments $\delta \times \delta'$. For a statistical distribution of ions with a mean concentration of n cm^{-3}, the mean deviation $|\overline{\Delta N}|$ from the mean value of the number of N ions in a volume δ^3 is given by

$$|\overline{\Delta N}| = |\overline{N - \bar{N}}| = \sqrt{\bar{N}/2\pi} = \sqrt{n\delta^3/2\pi} \qquad (2.\ 23)$$

The uniaxial energy $\delta^2 \, \Delta E_{\text{anis}} \; (y)$ (for wall position y) of the $N \; (y)$ anisotropic ions per volume element δ^3 in the wall with respect to the uniaxial energy in a domain must be calculated taking into account the $\sin^4 \theta$ term because the $\sin^2 \theta$ term used above cancels for equal population of the two types of sites with easy direction along the x-axis and z-axis. Thus we obtain

$$\text{E}_x \; (\theta) = \varepsilon_1 \cos^2 \theta + \varepsilon_2 \cos^4 \theta \qquad \text{(easy } x\text{-axis)}$$

$$\text{E}_z \; (\theta) = \varepsilon_1 \sin^2 \theta + \varepsilon^2 \sin_4 \theta \qquad \text{(easy } z\text{-axis)}$$

where θ is the angle of the magnetization direction with respect to the z-axis (c-axis) for which we use the approximation $\theta = \pi\eta/\delta$ in the wall. The wall energies per unit area is given by,

$$\delta^2 T_{\text{anis}}(\theta) = \int_0^{\alpha} N(y)\,(2\delta)^{-1}\,[E_x(\theta) + E_z(\theta) - E_x(0) - E_z(0)]\,d\eta = -1/8\,\varepsilon_2\,N(y) \quad (2.24)$$

Since $y = 0$ is an equilibrium position of the wall we have :

$$\Delta E_{\text{anis}}(y) = -0.12\,\varepsilon_2\,\delta^{-2}\,[N(0) + \Delta N y^2\,\delta^{-2}] = \text{const} + 0.12\,|\,\varepsilon^2\,\Delta N\,|\,\delta^{-4}\,y^2 \quad (2.25)$$

where $\Delta N = N(\delta) - N(0)$ is a quantity that will vary along the wall. The mean value of these differences $|\,\overline{\Delta N}\,|$ between the numbers of hard ions in adjacent cubic volume elements will be of the same magnitude as the mean deviation $|\,\Delta N\,|$. Using the approximation $|\,\Delta N\,| \simeq |\,\overline{\Delta N}\,|$ it follows that

$$\Delta E_{\text{anis}}(y) = \text{const} + 0.12\,(2\pi)^{-1/2}\,\varepsilon_2\,\delta^{-5/2}\,n^{-1/2}\,y^2 \equiv \text{const} + 1/2\,f\,y^2 \quad (2.26)$$

and this leads to

$$\Delta\mu^{-1} = lf\,(16\pi M_s^2)^{-1} = (64\times 1.4)^{-1}\,\pi^{-3/2}\,l\,|\,\varepsilon_2\,|\,n^{1/2}\,M_s^{-2}\,\delta^{-5/2} \quad (2.27)$$

where ε_2 is related to the cubic anisotropy constant K_1 according to $\varepsilon_2 = 9K_1/4$. This equation may be applied to the PME at 77 K in ferrous-doped YIG[4] using the values $l = 10^{-3}$ cm, $n = 10\times 10^{19}$ cm^{-3} (0.005 Fe^{2+}/mol), $M_s = 190$ gauss and $\delta = 500$ A. From the example of $\Delta\mu^{-1} = 0.04$ ($\mu = 160 \rightarrow 20$), we find 50 cm^{-1}/ion corresponding to a cubic anisotropy constant of $K_1 = 20$ cm^{-1} which is an acceptable value for Fe^{2+}.[5]

References

1) F. K. Lotgering : J. Phys. Chem. Solids 36 (1975) 1183.
2) K. Hisatake : "The basis of Ferrites and Magnetic Materials" (Gakken Pub. Co Tokyo, 1979. p. 79)
3) J. Smit and H. P. J. Wijn : "Ferrites" (John Wiley, New York, 1959).
4) U. Enz, R. Metselaar and P. J. Rijnierse : J. Physique 32 (1971) C1-702.
5) M. D. Sturge : Phys. Rev. 180 (1969) 402.

2. 2. Magneto-Optical Effects

2. 2. 1. Microscopic origin of optical absorption

Earlier studies of crystal-optical absorption in YIG[1~4] have been limited to absorption coefficients below about 0.25 eV because of sample-thickness limitations inherent in the use of bulk crystals. Wood et al.[1] have examined the region of the absorption edge between about 1.0 and 2.4 eV and have related their results to a superposition of crystal field [3d→3d within Fe^{3+}] and charge transfer [Oxygen (2p)→iron (3d)] as discussed earlier by Clogston and by Wicckersheim et al.[4] For assignment of various crystal field transitions the diagrams of crystal field levels for transitionmetal ions are being used.[6] They also found[1,3] that optical transmission for photon energies below the absorption edge near 1.2 eV could be improved substantially over the results of previous studies[2] by suitably adoping with such tetravalent ions as Si^{4+}. A series of doping experiments[3] involving both Si^{4+} and Ca^{2+} strongly suggested that the extra absorption tail in the infrared, observed in undoped crystals grown from a PbO-B_2O_3 flux, was related to the presence of Fe^{4+} ions in contrast to FZ (floating zone) YIG. An examination of Fe^{2+} -Fe^{4+} equilibrium in this system has been given by Nassau[7], Metselaar et al.[8] and one of the authors (K. H.).[9] And recently, Yokoyama et al.[10] has given a detailed study of impurity effects on the optical absorption loss of magneto-optical garnet crystals grown by liquid phase epitaxial method. Wood et al.[1~3] found the nearly quadratic dependence of the iron related absorption YIG on the total

ion content for concentrations above a few atomic percent, which implies that a simple view of optical transitions involving isolated and atomic like Fe^{3+} cannot be always valid. According to the energy band calculations of Mattheiss[16], one-electron 3d-states overlap sufficiently with relatively broad ($\simeq$ 4eV) oxygen-2*p* band to form broad Bloch-like 3d bands. This picture is no longer valid when the *d* states becomes partially filled as in the iron garnets. In these cases, electronic correlations become sufficiently important to condense the itinerant *d* electrons into highly correlated localized *d* states which resemble those of the free ion.[12] The localized *d* electron model is supported not only by the high resistivity of many transition metal oxides but also by the observation[13] that the many elecctron $3d$-$3d$ crystal-field transitions associated with Ni^{2+} in $Ni_xMg_{1-x}O$ occurs at almost precisely the same energies for all values of x. Similarly, many of the Fe^{3+} crystal field transition observed in YIG are also observed in yttrium gallium garnet (YGG) dilutely doped with Fe^{3+}. This localized view may be made compatible with the observation cited earlier that the strengths of iron-related optical absorptions in YGG (Fe^{3+}) increase almost quadratically with iron content. Clearly there are non-localized aspects to the iron 3d electrons, but we could have anticipated this result by noting the very large antiferromagnetic Fe-O-Fe exchange interaction in YIG. Besides, the spin-forbidden crystal field transitions are allowed with large oscillator strength by admixture of nearby, overlapping charge transfer transition of the type oxygen ($2p$) $\rightarrow$ Fe ($3d$). Kahn et al.[14] have discussed these transitions in some detail using a standard molecular orbital framework based on the earlier work of Clogston.[5] This method is useful in some cases, but fails to draw a clear distinction between band and localized states. To help clarify this important point, Adler et al.[15] have introduced the picture based on the split-density of state in their discussion of NiO. Figure 2.4 shows the Adler-Feinleid energy-level scheme for YIG on the basis of the above description.[15] One-electron band states are drawn to the left of a vertical line, while many electron *d* states, localizd by electronic correlation, are drawn to the right. Superscripts labeling each of the one-electron bands to the left refer to the total available number of electronic states per formula unit. The energy scale is relative, although it may be expected that the oxygen-2*p* band is about 4 eV wide[16], that the minimum $2p\rightarrow 4s$ separation is about 6-8 eV and that the width of the *d* band is about 3-4 eV. Schematically four main peaks in the density of states curve can be identified qualitatively with the molecular-orbital states forming the important components of the bands in these regions. The *e* and t_2 states are associated with tetrahedral Fe^{3+}, while the e_g and t_{2g} state refer to octahedrol Fe^{3+}. Also the relative energy positions shown are only illustrative at this point. Furthermore, it should be identified to particular iron sublattice. The transition A ($^6A_{1g}\rightarrow{}^4T_{1g}$) corresponds to the lowest band gap near 1.0 eV in the iron garnets, while the transition B ($^6A_1\rightarrow{}^4T_1$) produces an absorption peak 2.0 eV These are weak transitions, since they are spin forbidden and in the case of octahedral Fe^{3+}, they are also parity forbidden. As discussd by Kahn et al.[12], these forbidden transition, however, may be changed to the allowed one through a spin-orbit interaction and lattice distortions which combine to admix the nearby $2p\rightarrow 3d$ charge transfer bands. Electricdipole allowed transitions may occur from the filled oxygen-2*p* band to either the iron-*d* electron system or to the broad iron-4*s* band. In the former

case we have indicated a series of localized excitonic levels having the configuration $2p^5\ 3d^6$ lying just below a continum of bandlike d states labeled $3d$[15]. The excitonic states could involve nearest neighbour or possibly electron hole interactions at the next nearest neighbour and might even be unresolvable due to electron-phonon broadening. Optical transitions of the type $2p \rightarrow 3d$ are shown by arrows C and D. At higher energies than 8 eV, electric dipole allowed $2p \rightarrow 4s$ transions may be indicated by arrow E. These transitions are between the oxygen-$2p$ band and the Fe^{3+} and the $4s$ band. One of the authors [K. H.] has tried to ascribe these transitions to the PME (X-ray) as discussed in the next section.[16~18] Figure 2.5 (a) shows the typical absorption spectrum of YIG, around the photon energy ranges the PME concerns with mainly.[19] Figure 2.5 (b) shows the absorption spectrum of the rare earth iron garnets including YIG. So far the optical absorption characteristics has been mentioned mainly in garnets.[20] Next we turn to those properties in spinel ferrites. In Fig. 2. 6, the near infrared absorption spectral of severa spinel ferrites[20] are presented. The window between $0.15 \sim 0.4$ eV is clearly indicated though it is not so deep nor broad as in YIG. This may be at least partly due to several types of imperfections such as chemical non-stoichiometry, impurities and crystal defects. Previously one of the authors (K. H.) attributed to it the result that the intensity of PME in spinels is generally less than in YIG.[21] However, the optical absorption seems to be strongly influenced by the presence of octahedral or tetrahedral Fe^{2+} forming electronic charge carriers. Between region 1 and 2 eV, the transitions are usually identified and transitions between $3d$ levels split by the crystal field. For example, the steep increase of the absorption in $NiFe_2O_4$ at 1 eV was attributed to the Ni^{2+} crystal field transition $^3A^2 \rightarrow {}^3T^2$.[22] This peak can be observed in the spectrum of NiO (1.15μm) and also in a Faraday rotation dispersion of $NiFe_2O_3$.[20] Correspondingly, its energy should be equal to the crystal field splitting parameter $\Delta = 10\ Dq$. This transition, like all crystal field transitions in octahedrally coordinated ions, is parity-forbidden but may be allowed due to statical or dynamical violation of the local inversion symmetry. For tetrahedral cations, the parity restriction is not valid. On the other hand, the crystal field transitions in many cases including Fe^{3+} are also spin forbidden. The fact that in spite of the selection rules many of these transitions appear in the spectra cannot be well understood, although several models have been proposed. One of those models is that simultaneous excitation of a magnon allows this transition due to cancellation of ΔS_{tot}.[23, 24] Another model proposed by Clogston[5] is that the admixture of higher states via spin orbit coupling makes no longer a good quantum number and thus the spin constraint removed. But in most cases, this fails to account for the observed oscillator strength and some other effects[25]. To sum marize, the energy levels which are important in the megneto-optical properties of garnets with Fe^{3+} may be classified :

1) A filled valence band of oxygen $2p$ states.
2) Localized $3d$ states of Fe^{3+}. These are associated with octahedral and tetrahedral sites.
3) $3d$ band. These have density of state peak corresponding to the molecular orbits which are important components of the band state These peaks are identified as e and t_2 states of tetrahedral and e_g and t_{2g} of octahedral Fe^{3+}.

4) The 4*s* band may begin well above the lower edge of the 3*d* bands. The valence band is completely filled, while the crystal field levels are partly filled. Thus the lowest energy electronic transitions to be encounted are within the crystal field states. If only the single ion is considered, these are spin-forbidden since they involve reversing a spin. For octahedral sites they are in addition parity forbidden. Thus these lines are intrinsically very weak. At higher energies we expect very strong electric dipole allowed interband transitions $2p \rightarrow 3d$ and at much higher energies $2p \rightarrow 4s$. These are charge transfer transitions in which an electron would go from a state with 2*p* character to a 3*d* state. The situation is again pictorially shown in fig. 2. 7 in the simple way.

References

1) D. L. Wood and J. P. Remeika : J. Appl. Phys. 37 (1966) 798).
2) J. F. Dillon : J. Phys. Radium 20 (1959) 374.
3) D. L. Wood and J. P. Remeika : Appl. Phys. 38 (1967) 1038.
4) K. A. Wickersheim and R. A. Lefever : J. Chem. Phys. 36 (1962) 844.
5) A. M. Clogston : J. Appl Phys. 31S (1950) 198.
6) Y. Tanabe and S. Sugano : J. Phys. Sob. Japan 11 (1956) 864.
7) K. Nassau : J. Crys. Growth 2 (1968) 215.
8) R. Metselaar and M. A. H. Huyberts : J. Sol. Stat. Chem. 22 (1977) 309.
9) K. Hisatake : Trans. JPn. Inst. Met. 13 (1972) 305.
10) L. F. Matheiss : Phys. Rev. B5 (1972) 306.
11) Y. Yokoyama, N. Koshizuka and K. Ando ; Oyo Buturi 57 (1988) 1546.
12) D. Adler and J. Feinleıb : Phys. Rev. B2 (1970) 3112.
13) D. Reiner and B. Bunserges : Phys. Chem. 69 (1965) 82.
14) F. J. Kahn, P. S. Pershan and J. P. Remeika : Phys. Rev. 186 (1969) 891.
15) D. Adler and J. Feinleib : Phys. Rev. B2 (1970) 3112.
16) L. F. Mattheiss : Phys. Rev. B6 (1972) 4718.
17) K. Hisatake and T. Matsuyama : Jpn. J. Appl. Phys. 13 (1974) 2063.
18) K. Hisatake, K. Ohta, N, Ichinose and H. Yokoyama : phys. stat. sol. (a) 26 (1974) K79.
19) K. Hisatake. K. Ohta and Y. Noro : phys. stat. sol. (a) 30 (1975) K83.
20) U. Enz and H. van der Heide : Sol. Stat. Commun. 6 (1968) 347.
21) G. Zanmarchi and ₫. F. Bongers : J. Appl. Phys. 40 (1969) 1230.
22) K. Hisatake and K. Ohta : J. de Physique 38 C1 (1977).
23) C. J. Ballhausen : "Introduction to Ligand Field Theory" (McGraw-Hill Book Comp. Inc., New York, 1962).
24) C. Kittel : "Quantum Theory of Solids" (John Wiley & Sons, Inc. 1963, New York)
25) G. B. Scott : Proc. Int. School of Phys. "Enrico Ferm" ed., A. Paoletti (North-Holland, 1978) p. 445.
26) G. B. Scott, D. E. Lacklison and J. L. Page : Phys. Rev. B10 (1975) 971.

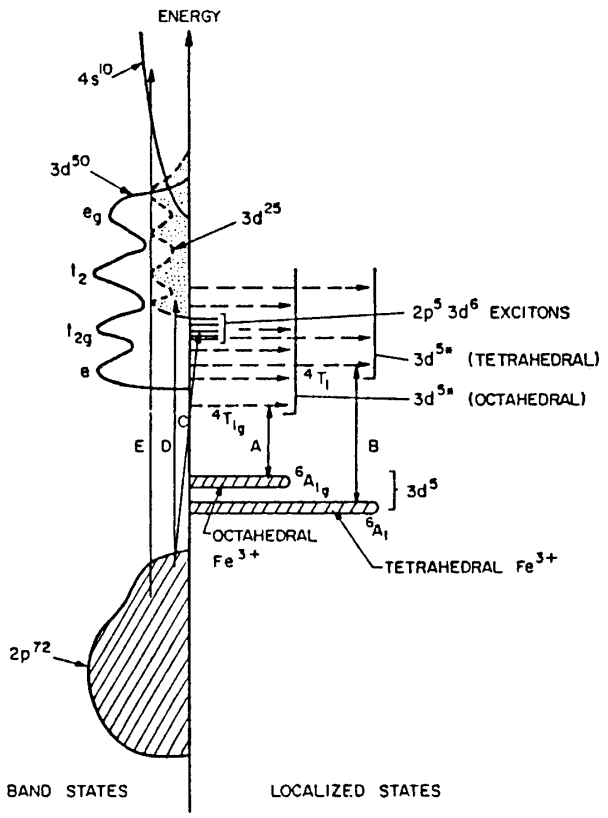

Fig. 2. 4 Proposed Adler-Feinleb energy-level scheme for iron garnets[14]. Band states are shown to the left, and localized states to the right. The superscripts on the bands refer to the number of states per formula unit.

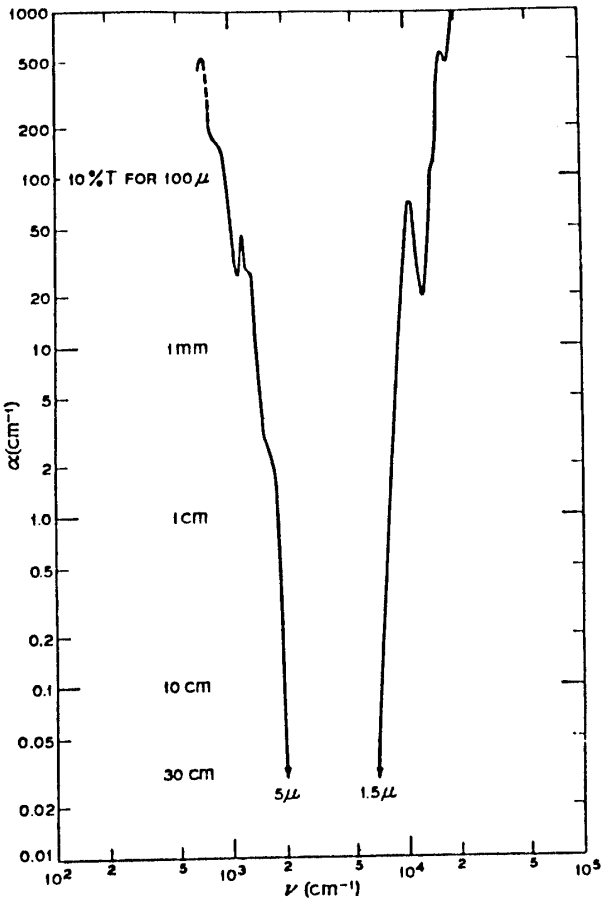

Fig. 2. 5 (a) Absorption coefficient of pure YIG between 6,000 and 20,000cm^{-1}. (0.7 eV-2.5 eV). The absorption is so low that only an upper limit could be established.[3]

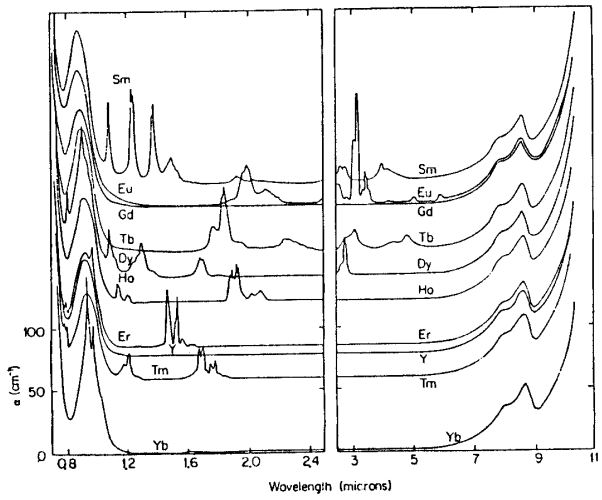

Fig. 2. 5 (b) Absorption spectrum of the rare earth iron garnets[3]

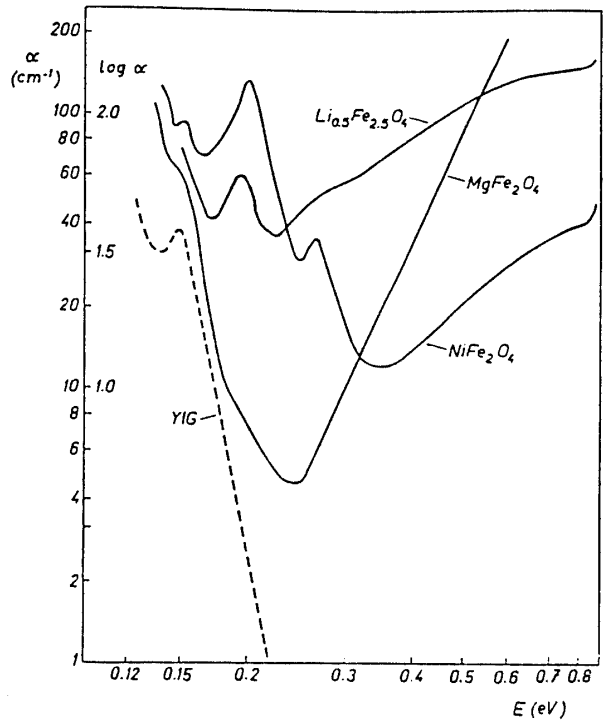

Fig. 2. 6 Near-infrared absorption spectra of several spinel ferrites.[20]

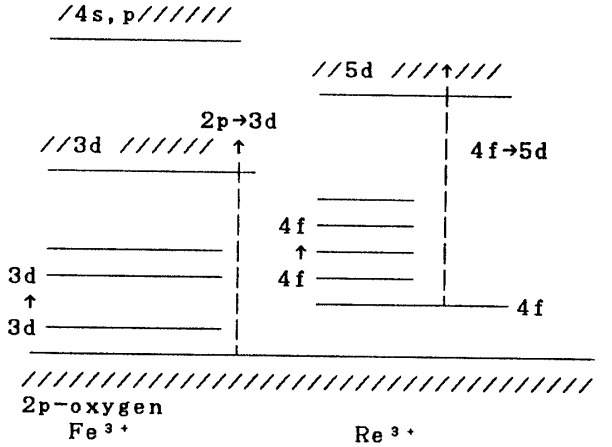

Fig. 2. 7 Simple representation of energy levels in YIG.

2. 2. 2 Irreversible optical absorption

Dillon et. al found an irreversible photoinduced change in the optical absorption constant of YIG (Si ; 0.018) on illumination of the sample with white light.[1,2] The absorption was sensed with a low intensity light beam having a photon energy of $E = 1.2$ eV. The result is shown in Fig. 2. 7 : the sample is first cooled down from room temperature to 15 K with little change in the absorption constant α. It is then illuminated with intense white light which brings down to $10cm^{-1}$. This change is irreversible except if the sample is brought back to high temperature : then increases gradually to its original value with increasing temperature, the process taking place between about 20 K and 200 K. This relaxation behaviour shows that after illumination the material is in a frozen state of high energy, which is identified with the high energy state as will be described afterwards, connected with our experimental results of imaginary part of permeability. Based on Enz's model, ferrous ion may be effectively moved to sites further from donors, with a high Coulomb energy. With increasing temperature, they relax back to sites near the donors. The experiment also gives evidence regarding the distribution of activation energies. If the recovery process is interrupted by cooling

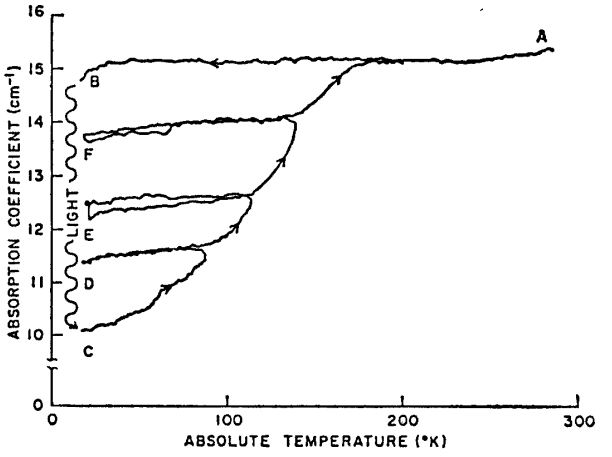

Fig. 2. 8 Absorption coefficient α at 1.15 μ of $Y_3Fe_{4.982}Si_{0.018}O_{12}$ as a function of temperature. Sample was cooled to approximately 15 K. Illumination with an intense white unpolarized light then produced a large decrease in α. This change in α could be progressively destroyed by heating the crystal to temperatures ranging up to 170 K.[1]

down again, no significant change in the absorption constant occurs. In each of be temperature cycles, a part of the original light induced change turns out to have relaxed. This is interpreted on the basis of an increase in activation energy of Fe^{2+} with distance from a donor. At a given temperature, all electrons within a given distance from a donor will be able to move fast enough to relax back to a donor under the influence of its Coulomb attraction. As the temperature increases, the distance increases, so that more and more ferrous ions recombine with donors, and more of the light-induced change is lost. In polycrystalline samples the rate of photoinduced change of several physical constants is strongly influenced by light scattering due to pores, in the same way as by a strong absorption, light influencing only a thin surface layer of the specimen and relaxation process[3,4], which seems to complicate the underlying mechanism as will be discussed afterwards again.

References

1) J. F. Dillon, E. M. Gyorgy and J. P. Remeika : J. J. Phys. (Paris) 32C1 (1971) 794.
2) E. M. Gyorgy, J. F. Dillon and J. P. Remeika : J. Appl. Phys. 42 (1971) 1454.
3) K. Hisatake : J. Appl. Phys. 48 (1977) 2971.
4) M. Pardavi-Horvath : Prog. Cryst. Growth Charact. 5 (1982) 175. (Continued ; Chap. 2)